Biophysical Journal Volume 94 March 2008 2423–2433

Phycocyanin Sensitizes both Photosystem I and Photosystem II in Cryptophyte *Chroomonas* CCMP270 Cells

Chantal D. van der Weij-De Wit,* Alexander B. Doust,* Ivo H. M. van Stokkum,* Jan P. Dekker,* Krystyna E. Wilk,† Paul M. G. Curmi,†‡ and Rienk van Grondelle*

*Department of Physics and Astronomy, Faculty of Sciences, Vrije Universiteit, 1081 HV Amsterdam; †School of Physics and Centre for Immunology, The University of New South Wales, Sydney, N.S.W., Australia; and ‡Centre for Immunology St. Vincent's Hospital, Sydney, N.S.W., Australia

ABSTRACT This article presents an investigation of the energy migration dynamics in intact cells of the unicellular photosynthetic cryptophyte *Chroomonas* CCMP270 by steady-state and time-resolved fluorescence measurements. By kinetic modeling of the fluorescence data on chlorophyll and phycocyanin 645 excitation (at 400 and 582 nm respectively), it has been possible to show the excited state energy distribution in the photosynthetic antenna of this alga. Excitation energy from phycocyanin 645 is distributed nearly equally between photosystem I and photosystem II with very high efficiency on a 100-ps timescale. The excitation energy trapping times for both photosystem I (~30 ps) and photosystem I (200 and ~540 ps) correspond well to those obtained from experiments on isolated photosystems. The results are compared with previous results for another cryptophyte species, *Rhodomonas* CS24, and suggest a similar membrane organization for the cryptophytes with the phycobiliproteins tightly packed in the thylakoid lumen around the periphery of the photosystems.

INTRODUCTION

Photosynthetic marine algae rely heavily on the ability to capture all wavelengths of visible light, not just those of chlorophyll (Chl) and carotenoids as in terrestrial species. Phycobiliproteins enable such a wider spectral window of absorption, and relating the location and energy transfer dynamics of antenna proteins to their function in intact algae is of interest. In this work, we show that phycocyanin excitations sensitize both photosystem I (PSI) and photosystem II (PSII) in the unicellular cryptophyte organism *Chroomonas* CCMP270.

Cryptophytes have a unique armory of light absorbing pigments (Chl *a*, Chl *c2*, the carotenoid alloxanthin) (1) in addition to uniquely possessing only a single type of phycobiliprotein (2). One of the most conspicuous features of cryptophytes is the location of the water-soluble phycobiliproteins distributed evenly across the lumen (3). In contrast, in cyanobacteria three types of phycobiliproteins combine to form so-called phycobilisomes, which are bound to the stromal side of PSII (4–7).

It has been shown that light absorbed by phycobilins and Chl *c2* is used preferentially to drive photochemical reactions at PSII in cryptophytes and cyanobacteria (8–15), where the energy transfer between phycobiliproteins and PSII in cryptophytes is extremely efficient (16,17). Bruce et al. (8) recorded an increased contribution of phycobiliproteins to the excitation spectrum of PSII with respect to PSI in several cryptophyte algae. Lichtlé et al. (9) suggested that the PSII antenna is composed of both phycobiliproteins and Chls, whereas PSI is provided with energy by Chls only (10), because spillover from PSII to PSI was shown to involve Chls only. This model strongly resembles that proposed by Mimuro et al. (11), wherein the excitation energy from PE545 is transferred to the Chl *a*/*c*2 light-harvesting complex that is bound to PSII. Thus, Chl *a*-containing antenna proteins are thought to be primarily responsible for funneling energy to PSI (1,9,12). However, transfer from phycobiliproteins to PSI in these organisms has not been ruled out (13). Absence of an energy transfer pathway from the phycobiliproteins to PSI in cryptophytes would be in contradiction with the observed even distribution of phycobiliproteins in the lumen (3). Based on a time-resolved study, we reported equally distributed energy transfer from phycoerythrin 545 (PE545) to both PSI and PSII for the cryptophyte species *Rhodomonas* CS24 (18). The ratio of PSII to PSI in cryptophytes is unknown and may be related to the growth conditions and thus also to the observations about preferential photosystem sensitization outlined above. There is, however, no consensus about the specific antenna composition of PSI and PSII.

Chroomonas CCMP270 relies on phycocyanin 645 (PC645) as its primary light-harvesting antenna (19,20). The structure of PC645 has been described briefly previously (21). PC645 is a $(\alpha_1\beta)(\alpha_2\beta)$ heterodimer containing one dihydrobiliverdin (DBV) and two phycocyanobilin (PCB) pigments on each β-subunit and one mesobiliverdin (MBV) pigment on each α-subunit (22). These bilins have absorption maxima at 585, 645, and 622 nm, respectively, resulting in a deep blue color of the organism. The fluorescence emission maximum is at 660 nm. These absorption wavelengths allow these algae to increase their photosynthetic efficiency and live at

Submitted May 31, 2007, and accepted for publication October 18, 2007.

Chantal D. van der Weij-De Wit and Alexander B. Doust contributed equally to this work.

Address reprint requests to Rienk van Grondelle, Tel.: 31-20-598-7930; Fax: 31-20-598-7999; E-mail: R.van.Grondelle@few.vu.nl.

Editor: Feng Gai.

0006-3495/08/03/2423/11 $2.00

doi: 10.1529/biophysj.107.113993

lower light-regimes and greater depths than most other (nonphycobiliprotein containing) algae. In the isolated protein, only one of the PCB bilins is the final acceptor of the excitation energy and is responsible for emission (23,24). A single emitting terminal bilin was also observed for isolated PE545 from *Rhodomonas* CS24 (24). In intact *Rhodomonas* CS24, however, it has been shown that energy transfer from the phycobiliproteins to the chlorophyll-containing proteins embedded in the thylakoid membrane can occur from any of the peripheral bilin chromophores (18).

A model for the organization of the thylakoid membrane of the cryptophyte *Rhodomonas* CS24 has been suggested (18), which shows some stacking of the membrane and segregation of PSI and PSII, as in higher plants, but has a wider lumenal space (25–27). PSI is most likely limited to the unstacked regions, whereas the Chl *a*/*c*2 light harvesting complex (LHC) may be located predominantly in the stacked regions of the thylakoids (3,28). Phycobiliproteins in cryptophyte algae are packed densely in the thylakoid lumen and are not expected to display a preferential orientation, neither relative to each other nor to the membrane (25). The energy-transfer pathways for excitations on phycobilins to the photosystems in cryptophytes have not been conclusively determined and it is not known if there is an intermediate or linker functionality in the energy transfer mechanisms from the phycobilins to the photosystem Chls. Various suggestions from the literature include Chl *c2* (18,25), colorless ''linker-like'' proteins (14,26) and the high concentration of phycobiliprotein in the lumen (29). MacColl et al. (30) calculated the spectral overlap between cryptophyte PC645 and Chl *a*. Direct energy transfer by the Förster mechanism was deemed more probable than transfer through Chl *c2*.

In this work, we investigate the energy migration dynamics in intact cells of *Chroomonas* CCMP270 at physiological conditions using steady state and time-resolved fluorescence measurements. By kinetic modeling of the coupled time-resolved data from photosystem and phycocyanin excitation, it is determined that energy is transferred from PC645 about equally to PSI and PSII at a timescale of 100 ps.

MATERIALS AND METHODS

Sample preparation

Cryptophyte *Chroomonas* sp. (CCMP270 strain, National Culture Collection of Marine Phytoplankton, Bigelow Laboratory for Ocean Sciences, West Boothbay Harbor, ME) was cultured at 20°C under constant low light illumination (12 V white fluorescent tubes, 300 Lux at 0.3 m) in a modified ''Fe'' medium (31) under continuous aeration. Under these constant low light conditions, *Chroomonas* CCPM270 algae produce high levels of Phycocyanin. Contamination was inhibited by filtering the medium with 0.22-μm paper filters and the air supply with a cotton filter. The algae were sealed in bottles and sent from Sydney to Amsterdam in darkness, during which algal growth continued (32). During the experimental period, the algae were kept illuminated at constant temperatures and the bottle shaken daily to ensure sufficient air supply. Emission spectra of the algae taken daily over the course of the experimental period yielded the same result each time.

PC645 was isolated from *Chroomonas* CCMP270. The algal cells were harvested through centrifugation at 800 $\times$ *g* for 20 min at 4°C. The cell pellets were then re-suspended in twice their volume of a buffer at neutral pH and they were homogenized using a Teflon glass homogenizer. The cells were disrupted by French press (1000 psi, twice). The resultant solution was centrifuged at 23,000 $\times$ *g* for 1 h at 4°C producing a pellet containing the thylakoid membranes and other insoluble cell debris, and a supernatant solution containing the soluble portion of the cell including PC645. PC645 was isolated from ~50 ml of the supernatant using gradual ammonium sulfate precipitation from 0 to 80%. At each stage (0–50%, 50–60%, 60–70%, and 70–80%) the appropriate amount of ammonium sulfate (33) was added to the protein solution that was stirred gently on ice for 1 h. After each stage the solution was centrifuged at 23,000 $\times$ *g* for 30 min at 4°C, and the supernatant was used for the next stage. The PC645 content after each stage was determined using UV/visible spectroscopy (Cary 1 Bio, Palo Alto, CA). It was found that the pellets from the 60–70% stage contained the majority of PC645. The pellets were resuspended in 25 mM Hepes pH 7.5. Further purification was continued in a 4°C cold room through a BioLogic work station (Bio-Rad, Regents Park, NSW, Australia) using a combination of an ion-exchange column (HiLoad 26/10Q Sepharose, Amersham, Piscataway, NJ) and a size-exclusion column (HiLoad 26/60 Superdex, Amersham). UV/visible spectroscopy coupled with electrophoresis was used to confirm the purity and character of the final product. Fractions consisting of pure PC645 were concentrated using a 10 kDa Amicron Ultra-15 Centrifugal Filter Unit and snap frozen using liquid nitrogen before being stored at −80°C.

Spectroscopy

Absorption spectra were recorded using a Cary 100 absorption spectrophotometer. Fluorescence emission and excitation spectra were recorded on a Jobin Yvon Fluorolog-3-11 fluorometer (Edison, NJ) in right angle mode. Algal cells were diluted with artificial seawater and PC645 was diluted with 25 mM Hepes pH 7.5 to an optical density of 0.05 cm^{-1} for fluorescence measurements. For the 77 K measurements, glycerol (60% v/v) was added as a cryoprotectant and a nitrogen cryostat (Oxford, Abingdon, UK) was used.

Time-resolved fluorescence measurements were made using a streak camera setup that has been described previously (34), including details on the data acquisition and analysis. The samples were magnetically stirred in a 1 cm quartz cuvette and cooled to 16°C. A total of 582 nm excitation pulses (150 fs) were generated using a Ti:sapphire laser (VITESSE, Coherent, Santa Clara, CA), a regenerative amplifier (REGA, Coherent), and a double-pass optical parametric amplifier (OPA-9400, Coherent) with subsequent interference filter (FWHM 15 nm). Four hundred nm pulses were generated using the frequency doubled fundamental from the Ti:sapphire laser. The repetition rate was 150 kHz, and the pulse energy 0.5 nJ. The excitation polarization was tuned vertical, using a Berek compensator. The excitation light was collimated with a 15-cm focal length lens, resulting in a focal diameter of 150 μm in the sample. The fluorescence was collected under right angle with the excitation light and the cuvette positioned in the front face mode. The fluorescence was measured after passing through a red sharp cutoff glass filter at magic angle using a Chromex 250IS spectrograph and a Hamamatsu C5680 synchroscan streak camera. The streak images were recorded with a cooled, Hamamatsu C4880 CCD camera. Typically, three scans of 30-min per refreshed sample were collected and averaged. The streak images measure 315 nm in the spectral domain and were collected at different timebases of 200, 500, and 2000 ps. The time-resolution of the experiments was 5 ps.

The data were subjected to global analysis, in which a sum of exponential decays are fit to the fluorescence, which result in decay associated spectra (DAS). DAS can be interpreted as the loss or gain of fluorescence with a certain lifetime, as illustrated by the positive or negative amplitude in the spectra. In the target analysis, a kinetic model is fit to the data, which results in species associated spectra (SAS). A detailed description of global and target analysis can be found in Van Stokkum et al.(35,36).

RESULTS AND DISCUSSION

Absorption

The absorption spectra of *Chroomonas* CCMP270 algae at room temperature and 77 K are shown in Fig. 1, as well as the 77 K absorption of isolated PC645. The second derivative spectrum of the 77 K algae trace (see *inset*) allows for the characterization of the Chl, carotenoid, and phycocyanin bands (11,37–39). Chl *a* has its Q_Y absorption maximum at 682 nm and a band at 443 nm in the Soret region. The Chl *c2* Soret band is seen at 468 nm, however its Q_Y absorption (~640 nm) is masked by the absorption peaks of PC645 at 585, 622, and 645 nm, respectively corresponding to the DBV, MBV, and PCB bilins (23). The carotenoids, mainly alloxanthin, absorb around 500 nm.

Emission and excitation

The emission spectra of *Chroomonas* CCMP270 algae have been recorded both at room temperature and 77 K for a range of excitation wavelengths. The resulting spectra are shown in Fig. 2 *a* and the emission of isolated PC645 at room temperature and 77 K in Fig. 2 *b*. At room temperature (*solid lines*), PC645 emission is observed at 664 nm and Chl *a* emission at 683 nm. The energy transfer from PC645 to the Chls of the photosystems becomes evident from the Chl *a* emission, which has comparable amplitude on 420 and 580 nm excitation, although Chl *a* is known to have very minor absorption at 580 with respect to 420 nm. The energy transfer from PC645 to photosystem Chl *a* is also clearly confirmed in the excitation spectra (not shown). The Chl *a* emission is observed to increase on shifting the excitation wavelength from 500 to 420 nm, conform the increasing absorption strength of the Chls *a*.

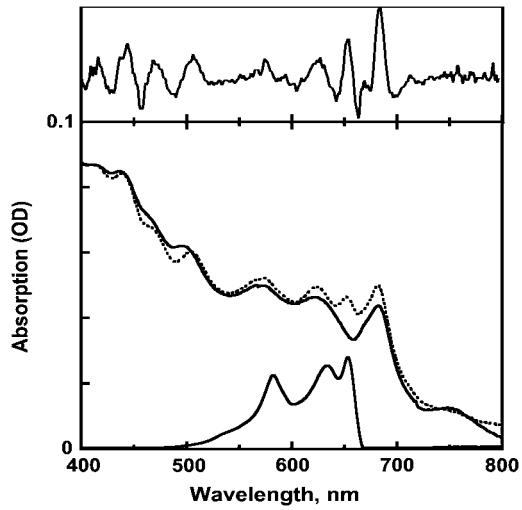

FIGURE 1 Room temperature (*solid*) and 77 K (*dotted*) absorption spectra of *Chroomonas* CCMP270 algal cells. The negative of the second derivative of the 77 K trace is shown at the top. The 77 K absorption spectrum of isolated PC645 is shown at the bottom of the figure (*solid*).

The emission maximum of isolated PC645 is at 660 nm at room temperature (Fig. 2 *b*), which is blue-shifted with respect to the emission maximum of PC645 in the intact cells (664 nm, Fig. 2 *a*). A similar observation was made in *Rhodomonas* CS24 (18). Tight packing and PC645 to PC645 excitation energy transfer of the water-soluble phycobiliproteins in the thylakoid lumen might induce this red-shift of the emission. At room temperature, the efficiency of energy transfer from PC645 to the membrane Chls is observed to be higher in *Chroomonas* CCMP270 than was recorded for PE545 in *Rhodomonas* CS24 (18), as is concluded from the higher phycobiliprotein/Chl *a* emission ratio for the latter assuming similar fluorescence quantum yields for the two types of phycobiliproteins. This might be explained by the increased spectral overlap between PC645 emission (664 nm) and Chl *a* and Chl *c* absorption (670 and 630 nm, respectively), with respect to that of PE545, which has its emission maximum at 585 nm.

A comparison of the emission spectra of *Rhodomonas* CS24 and *Chroomonas* CCMP270 also shows respective Chl *a* emission maxima of 686 and 683 nm (24). The blue-shift of the Chl *a* emission in *Chroomonas* CCMP270 with respect to *Rhodomonas* CS24 may indicate a spectrally slightly different PSII antenna in *Chroomonas* CCMP270, because PSI hardly shows emission at room temperature with respect to PSII (40).

At 77 K (*dotted lines*), a single Chl *a* emission band is observed with a maximum at 685 nm. The contributions of respectively PSI and PSII to this emission band cannot be discerned. However, PSI is known to show characteristic emission bands in the range 715–730 nm (different cryptophytes) (11) at 77 K, due to the presence of Chls with absorption wavelength longer than the primary electron donor of PSI, P700. Because PC645 also has vibrational emission bands in this spectral region (Fig. 2 *b*), it is very difficult to ascertain the possible presence of a small amount of red Chl *a* pigments in PSI. The characteristic second emission band of PSII at 695 nm at 77 K (41) is also absent in the spectra of Fig. 2 *a*. The latter observation might imply a different composition of cryptophyte PSII with respect to that of plants, cyanobacteria, and other algae.

At 77 K, the ratio of PC645 versus Chl *a* emission is observed to increase significantly, yet a small shoulder of Chl *a* emission is still visible at 580 nm excitation. The reason for the increase in emission intensity is the increase in the fluorescence yield of PC645 at lower temperatures. Consequently, only a minor fraction of free PC645 complexes in the cells will result in a large emission signal at 77 K. Again, the Chl *a* emission is observed to increase on shifting the excitation light from 500 to 420 nm, conform the Chl *a* absorption spectrum. Chl *c2* emission is degenerate with PC645 emission so its role, if any, in the transfer of PC645 excitations to the photosystems is difficult to

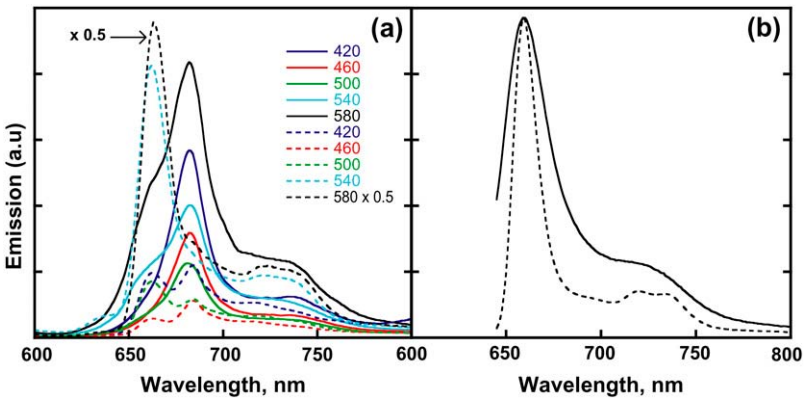

FIGURE 2 (*a*) Emission spectra of intact *Chroomonas* CCMP270 cells at room temperature (*solid*) and 77 K (*dotted*) at different selected excitation wavelengths. Note that the 77 K, 580 nm excitation spectrum has been halved to fit in the plot. PC645 emission maximum is at 664 nm and chlorophyll emission is at 683 nm. (*b*) Emission spectra of isolated PC645 at room temperature (*dotted*) and 77 K (*solid*) on 630 nm excitation, with maxima at 660 nm. The spectra have not been normalized to the excitation intensities.

determine as its emission will be masked by the emission of PC645 (37). In addition, Chl *c2* is known to transfer energy efficiently to Chl *a* (37), and is thus not likely to be observed in these fluorescence experiments.

Time-resolved fluorescence

The fluorescence decay of isolated PC645 was measured on 582 nm excitation and of intact algae on both 400 and 582 nm excitation at room temperature. At 400 nm the Chls of the photosystems are preferentially excited whereas at 582 nm PC645 is dominantly excited. The three datasets allow for a detailed kinetic analysis of both PC645 energy transfer and trapping, including the energy transfer from PC645 to the Chls in the membrane-embedded photosystem complexes.

Global analysis

The kinetic data were independently subjected to global analysis, resulting in the DAS displayed in Fig. 3, *a–c* for the three experiments. For PC645, fluorescence decay times are estimated of 2, 20, and 1380 ps (Fig. 3 *a*). At 582 nm excitation, the blue-most absorbing DBV pigments in PC645 are dominantly excited, which transfer their energy within the PC645 heterodimer to the red-shifted MBV and PCB bilins (23). Energy transfer is observed to occur on a 2-ps timescale indicated by the DAS that shows positive amplitude at 638 nm and negative amplitudes at 663 and 736 nm. It cannot be concluded, however, between which bilins the energy transfer occurs, although the 2-ps decay has been observed before at 585 nm excitation, and was assigned to the internal conversion between the high- and low-energy exciton states of the DBV dimer (42). The second DAS, with a previously observed lifetime of 20 ps (42; see also 49) also indicates energy transfer in PC645, with loss of 654 nm emission and gain at 672 nm, and likely represents energy transfer between the two terminal PCB bilins (23). The very small amplitude of this phase expresses how the fluorescence decay and rise of these spectrally similar components cancel. The timescale of this energy transfer step was difficult to determine, because good fits were obtained for a range of energy transfer timescales from 15 to 40 ps. This possible variance might indicate the presence of a range of energy transfer pathways within PC645 or between different PC645 proteins in the solution, leading to a spread of lifetimes. The final DAS has an overall positive amplitude with maximum at 661 nm and decays on the 1380 ps timescale, which is known to be the fluorescence lifetime of PC645 (42,43).

Global analysis of the intact algae excited at 400 nm resulted in fluorescence decay times of 37, 165, and 528 ps (Fig. 3 *b*). Both the 37 and 528 ps DAS show typical Chl *a* emission spectra, with respective emission maxima at 684 and 687 nm. The observed spectral shift between these two DAS can be explained by different origins (PSII or PSI). The 528 ps decay of emission at 684 nm is typical for PSII (43–46) with closed reaction centers, whereas PSI emission is

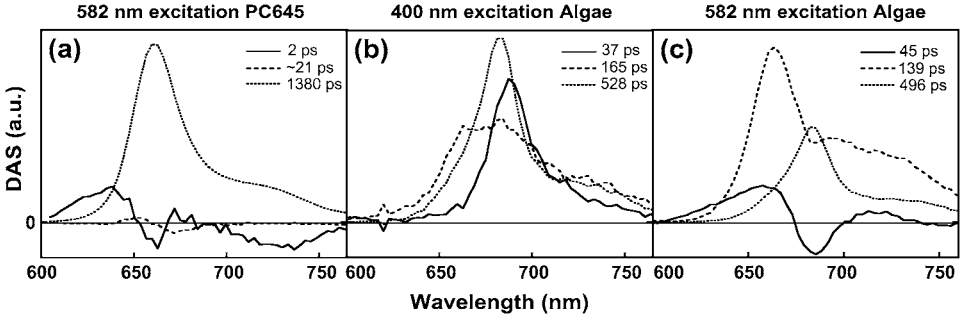

FIGURE 3 DAS of the global analyses of isolated PC645 excited at 582 nm (*a*), intact *Chroomonas* CCMP270 algae excited at 400 nm (*b*), and at 582 nm (*c*), respectively.

known to have decayed already by 150 ps (47–50). Consequently, the 528 ps DAS is assigned to PSII and the red-shifted 37 ps DAS to PSI. The 165 ps DAS shows additional decay amplitude at the blue-edge of the photosystem emission spectra. The extra amplitude is assigned to PC645. As a result, the 165 ps timescale indicates a mix of energy transfer from PC645 to the photosystems and trapping of excitations by charge separation in the reaction centers of the photosystems. It is concluded that PC645 has some absorption strength at 400 nm at room temperature (43).

The fluorescence decay of the intact algae excited at 582 nm could also be well described by three fluorescence decay times, 45, 139, and 496 ps, respectively (Fig. 3 *c*). The DAS corresponding to the 45 ps decay time shows positive amplitude at 657.5 nm and negative amplitude at 685.5 nm, indicative of energy transfer from PC645 to Chl *a*. The positive amplitude at 657.5 nm corresponds to the emission maximum of isolated PC645. Note that the 20 ps DAS from the isolated PC645 emission decay (Fig. 3 *a*) has negative amplitude at 672 nm, which is blue-shifted with respect to the negative maximum in intact algae at 685.5 nm. It can thus be concluded that energy transfer from PC645 to Chl *a* occurs on the 45 ps timescale. The decay time of the second DAS, 139 ps, is close to the value estimated on 400 nm excitation of intact algae (165 ps, Fig. 3 *b*). The 139 ps DAS shows an emission maximum at 663.5 nm, indicative of fluorescence of PC645, with a broad emission shoulder at higher wavelengths, indicative of fluorescence of the photosystems. Consequently, the 139 ps DAS describes energy transfer from PC645 to the photosystems and the simultaneous emission decay from these photosystems. The third DAS with emission maximum at 683 nm and lifetime of 496 ps has a clear lineshape and lifetime characteristic of PSII (44–47) and corresponds very well with the 528 ps lifetime derived from the 400 nm global analyses. It is thus shown that the excitation energy on PC645 becomes quenched by the photosystems, because the fluorescence lifetime of isolated PC645 is 1.4 ns.

Although energy transfer from PC645 to the Chls of the photosystems can be concluded to occur from these global analyses, the respective contributions to PSI and PSII cannot be determined. To resolve the PC645 and Chl kinetics in the intact algae, and to gain better understanding of this complex system, we applied a target analysis.

Target analysis

In target analysis, the algal fluorescence data are fit with a minimal kinetic model. Three fluorescent species are distinguished: PC645, PSI, and PSII, each with a characteristic SAS. Note that in the global analysis of the intact algae, each DAS consists of linear combinations of the SAS of PC645, PSI, and PSII (35,36). Fluorescence of these three species evolves multi-exponentially. In a target analysis, we aim to resolve realistic SAS in combination with a plausible kinetic scheme. Spectral constraints are used to increase the understanding of the kinetics under study, because they allow better estimation of the time-constants and are also often necessary due a to limited signal/noise (S/N) ratio of the data. The SAS of the three species were compared with steady state results and literature data. The photosystem kinetics are deliberately restricted and therefore the PSII decay lifetimes are represented by a two-component decay. These decays will be the weighted average of all the (complex) kinetic decays that are inherent to PSII, but had to be restricted to two components to make the analysis manageable.

The kinetic data on 400 and 582 nm excitation emphasize different aspects of the system. From a comparison of the absorption spectra of intact algae and of isolated PC645 (not shown), the contribution of PC645 to the absorption at 400 nm of intact algae was estimated to be $<15\%$. With 400 nm excitation, energy transfer from PC645 to the photosystems is thus less important than direct excitation of the photosystems, and therefore these data allow for a reliable estimation of the fast PSI kinetics. In addition, because so little PC645 is excited with 400 nm excitation, its ultrafast dynamics cannot be resolved. On the other hand, with 582 nm excitation, PC645 is dominantly excited and both the ultrafast relaxation (2 ps) in PC645 and energy transfer from PC645 to the photosystems are confirmed (see below). The target analyses of these two experiments were largely consistent.

The kinetic model fit to the 400 nm data is shown in Fig. 4 and its associated rate constants are collated in Table 1. Because PC645 emission is very minor on 400 nm excitation (Fig. 2) and is overlapped to a large extent by Chl emission, it is difficult to discern the small PC645 contribution from the total emission decay. To this end, we took the PC645

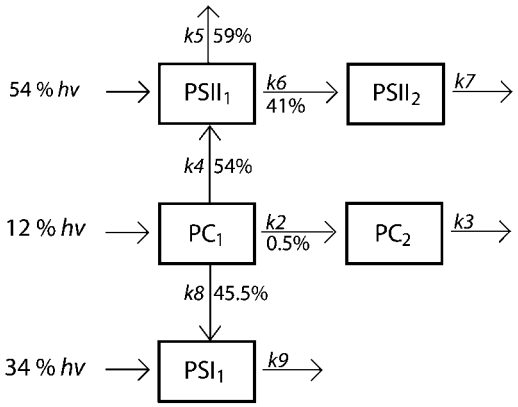

FIGURE 4 Target analysis scheme for the intact *Chroomonas* CCMP270 algae on 400 nm excitation. Three species are distinguished, PC645, PSI, and PSII, where a biexponential decay was necessary to describe both PC645 ($PC_{1,2}$) and PSII ($PSII_{1,2}$) kinetics. The fluorescence lifetimes that result from this kinetic scheme are 40, 100, 200, 518, and 1400 ps. The percentages reflect the energy distribution from the PC_1 and $PSII_1$ states. The ratio of PSII:PC645:PSI initial excitation was estimated to be 54:12:34. The rate constants associated with this target scheme are given in Table 1 and the decay associated amplitude matrix of the model is given in Table 2.

TABLE 1 Rate constants associated with the target models of Fig. 4 (400 nm) and Fig. 6 (582 nm)

Rate constant, ns^{-1}	400 nm	582 nm
k1	–	500
k2	0.0509	0.0509
k3	0.714	0.714
k4	5.18	5.18
k5	2.95	3.47
k6	2.04	1.67
k7	1.93	1.80
k8	4.39	4.39
k9	25.1	55.6

Estimated error is 10%.

spectral line-shape with 1.4 ns lifetime, resulting from the global analysis of the isolated PC645 (Fig. 3 *a*) and used it as additional a priori spectral information in the analysis of the 400 nm data, with a weight that was fine tuned in the fitting process. We took into account the spectral red-shift (4 nm) of PC645 fluorescence on incorporation into the cell (Fig. 2). As inferred from the global analysis (Fig. 3), the fluorescence decay of isolated PC645 could be fit with an evolution through three emitting states. Note that these are not real emitting states (35), but serve to describe the recorded fluorescence decay of PC645. However, although the emission of isolated PC645 was observed to evolve spectrally on a 2-ps timescale (Fig. 3), no attempts were made to resolve this fast component in the 400 nm target analysis due to the small PC645 emission signal with respect to the S/N ratio of the data. The 1.4 ns fluorescence lifetime of PC645 was a fixed parameter of the fit. Energy transfer branching to the photosystems was allowed for from the first PC645 emission state only, and for simplicity, the energy transfer from PC645 to a photosystem is described by a connection to the first compartment of that photosystem. An increased number of intermediate PC645 states did not improve the fit. Similarly, the PSII fluorescence kinetics could be well described by a biexponential decay, whereas a single decay sufficed to describe the PSI kinetics.

PSI and PSII decay kinetics are very complicated, as the many publications on isolated photosystems have shown (43–50). Indeed, multiple decay components with a variety of lifetimes are observed in PSII, both with open and closed reaction centers, and arise from energy transfer times convolved with charge separation and multiple electron transport steps including charge recombination. In such experiments on isolated photosystems, more than two lifetimes are often needed to satisfy the data analysis. In one such example of complex decay kinetics in PSII BBY preparations (47), various models are discussed that have been presented in the literature as descriptive of energy transfer and charge separation times. In our analysis, deriving the energy transfer rate and ratio of PC to PSI and PSII was of greatest importance. As such, all PSI and PSII decay lifetimes are summarized as one and two component decays, respectively. These decays will be the weighted average of all the (complex) kinetic decays that are inherent to PSII, but were restricted to two to make the analysis more manageable. Equally important, it was found that introducing more decay components did not improve the fit and no spectral evolution was needed for the photosystems.

For the 400 nm excitation, the initial excitation ratio of PC645, PSI, and PSII was estimated to be 12:34:54. As a consequence of the very small emission signal of PC645 and high spectral congestion of the PSI and PSII spectra, it was not possible to estimate the energy transfer ratio from PC645 to respectively PSI and PSII. The energy transfer ratio will not influence the resolved PSI and PSII spectra to a high extent, because these are dominantly populated by direct excitation. The energy distribution ratio from PC645 can be estimated in the kinetic analysis of the 582 nm data set, which results in ~45:55 (±10% relative standard error) for PSI and PSII respectively and these numbers were fixed parameters in the 400 nm fit.

The fluorescence lifetimes resulting from the kinetic model of Fig. 4 are 100 and 1400 ps for PC645, where energy transfer occurs to both photosystems on the 100-ps timescale. The fluorescence lifetime determined for PSI is 40 ps. The overall trapping of the excitation energy occurs in PSI core complexes in 20–60 ps (48–51) depending on the amount of red pigments, which is estimated to be low in the case of *Chroomonas* CCMP270 (Fig. 2). The light-harvesting antenna (LHCI) surrounding the PSI core has been shown to result in a second excitation decay time of maximally 130 ps (48), which also depends on the amount of red Chls present. Consequently, 40 ps is a plausible decay time for PSI, in particular for a PSI-LHCI system with a small amount of red Chls in LHCI (51). Sixty percent of the excitations on PSII are found to become trapped at a timescale of 200 ps and the other 40% is transferred to a long-lived trapping state with a lifetime of 518 ps. In higher plants, PSII was found to decay with time constants of 80 and 250 ps (47), where timescales longer than 250 ps arise due to closure of the PSII reaction centers (46). The observed timescales of 200 and 518 ps in this study are thus plausible PSII decay times when a proportion of PSII exist with closed reaction centers in the algae. Note how the determined lifetimes in the target analysis are in agreement with those estimated in the global analysis (Fig. 3 *b*). The SAS corresponding to the model of Fig. 4 are shown in Fig. 5, with respective emission maxima for PSI, PSII, and PC645 at 688.5, 683, and 664 nm. The excitation ratio of PSI and PSII has been adjusted to result in similar areas of their SAS, reflecting the fact that they bind the same Chl *a* pigment in both systems (35). The resolved PSII spectrum largely resembles that of PSII of higher plants. The PSI emission spectrum is clearly red-shifted with respect to that of PSII and has lower intensity on the red edge, which is consistent with the results of the similar cryptophyte alga *Rhodomonas* CS24, in an earlier experiment (18). The latter observation

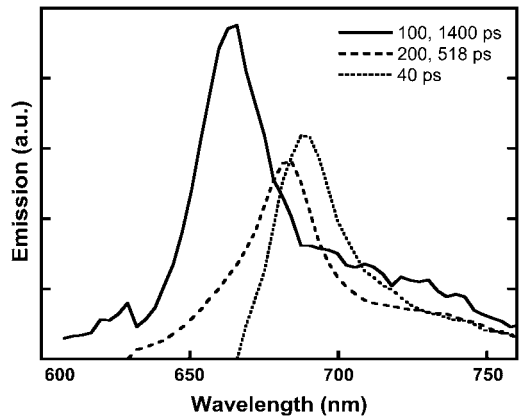

FIGURE 5 Species-associated spectra of *Chroomonas* CCPM270 on 400 nm excitation according to the model in Fig. 4. The solid line represents the emission of PC645 (664 nm), the dashed line PSII (683 nm), and the dotted line PSI (688.5 nm).

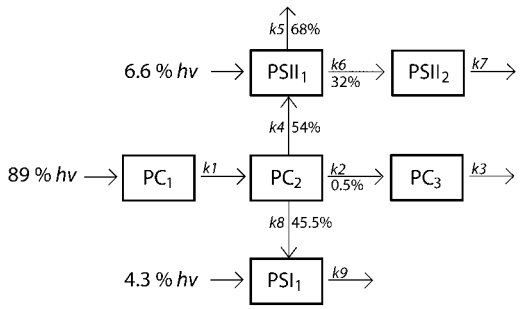

FIGURE 6 Target analysis scheme for the intact *Chroomonas* CCMP270 algae on 582 nm excitation. Three species are distinguished. PC645 is best described by three compartments as inferred from the global analysis. PSI and PSII are each described by one and two compartments, respectively. The fluorescence lifetimes that result from this kinetic scheme are 2, 16, 100, 193, 556, and 1400 ps. The percentages reflect the energy distribution from the PC_2 and $PSII_1$ states. The ratio of PC645:PSII:PSI initial excitation was estimated to be 89:4.3:6.6. The rate constants associated with this target scheme are given in Table 1 and the decay associated amplitude matrix of the model is given in Table 3.

confirms the near absence of typical red pigments in PSI of *Chroomonas* CCMP270.

Table 2 displays the decay associated amplitude matrix calculated from the model in Fig. 4. PC645 is observed to transfer energy to PSI and PSII on a 100 ps timescale. PSI decays on a faster timescale (40 ps) than it becomes populated through PC645 (100 ps). This is expected to result in so-called inverted kinetics with a negative amplitude (population rise) at a 40-ps timescale and positive amplitude (population decay) with a 100-ps time constant. However, the large contribution of direct PSI excitation (34%) results in a large positive amplitude with a 40-ps time constant. Consequently, the transfer from PC645 to PSI as shown in Fig. 4 is masked in Table 2 due to the significant direct excitation of PSI.

For the fluorescence data recorded on 582 nm excitation of the algae, the same kinetic model as presented in Fig. 4 was applied and a third compartment was added for PC645 to describe the fast (2 ps) energy relaxation within this complex (Fig. 6). Due to the limited S/N ratio, it was difficult to resolve the PSI kinetics in this experiment because of the high spectral overlap of the three species (PC645, PSI, PSII).

TABLE 2 Amplitude matrix for the different lifetimes associated with the target model of Fig. 4

	PC_1	PC_2	$PSII_1$	$PSII_2$	PSI_1
τ (ps)	0.12 *hv**	–	0.54 *hv**	–	0.34 *hv**
40	–	–	–	–	0.30
100	012	−0.0007	−0.14	0.04	0.04
200	–	–	0.68	−0.45	–
518	–	–	–	0.41	–
1400	–	0.0007	–	–	–

Negative amplitude indicates a rise of excited state population and a positive amplitude a decay.

*Indicates the initial excitation ratio of the PC_1, PSI_1, and $PSII_1$ compartments.

More importantly, because the excitations become trapped on PSI on a smaller timescale (40 ps) than population of PSI occurs through PC645 (100 ps), this energy transfer step is easily overlooked. Therefore, the PSI and PSII spectra found in the 400 nm target analysis were chosen as a priory information as well as the PC645 spectrum with 1.4 ns lifetime from the time-resolved measurement on isolated PC645 (Fig. 3 *a*), each of them with a weighting that was fine tuned. The initial excitation ratio was estimated to be 89:4.3:6.6 between PC645, PSI, and PSII, in good agreement with the relative absorption of PC645 and Chls in the algae at 582 nm.

The resulting fluorescence lifetimes are 2, 100, and 1400 ps for PC645, where spectral evolution was allowed for on the 2-ps timescale. For PSI a lifetime of 16 ps is found, which is smaller than that estimated in the 400 nm experiment and slightly faster than that normally observed for PSI cores. This will be due to the intrinsic uncertainty of this analysis, where PSI traps energy on a faster timescale than it becomes populated through PC645 and where PC645, PSI and PSII show significant spectral overlap. The red shoulder on the PC645 SAS can be explained by the local high concentration of PC645 proteins in the thylakoid lumen, leading to self-absorption effects. PSII fluorescence is found to decay biexponentially on timescales of 193 and 556 ps. These time scales are in accordance with literature values on PSII when a part of the PSII exists with closed reaction centers in the algae (44–47). The trapping ratio of excitations by these two phases is now 68:32, which was 60:40 for the 200 and 518 ps components in the 400 nm experiment. Note that the contribution of closed PSII reaction centers can differ between the two experiments. Consequently, the fraction of excitations trapped at the larger PSII decay time (~540 ps) may vary, with relatively more closed reaction centers in the 400 nm data than on 582 nm excitation, although it is noted that

these trapping ratios are within the 10% relative standard error of each other. The estimated fluorescence lifetimes in this target analysis are in agreement with those estimated in global analysis (Fig. 3 *c*).

The SAS corresponding to the 582 nm data are shown in Fig. 7. The 2-ps component has a maximum at 662.5 nm, with increased intensity on the blue edge with respect to the subsequent PC645 decay phases, which have emission maxima at 664 nm. The PC645 SAS are observed to have a rather pronounced red shoulder, which was absent in both the 400 nm data and that of isolated PC645. From Fig. 5, it is observed that 0.5% of the excitations remain on PC645 and decay with its fluorescence lifetime. In the fit, the PC645 spectrum is thus estimated from a very small amount of excitations. The resulting uncertainty in the determined SAS is expressed by the red shoulder. The loss of 0.5% of the initial excitations, highlights how efficient the light-harvesting process is in this organism. This loss is smaller than estimated for *Rhodomonas* CS24 (2%), which is in agreement with their steady-state emission spectra showing different phycobiliprotein/Chl *a* emission ratios. The PSII SAS peaks at 683.5 nm and the PSI SAS at 686.5 nm. Even though the model of Fig. 6 fits the data very well, it can be seen that the PSII spectrum still has a little shoulder at 664 nm. These observations illustrate how well connected PC645 and PSII are in this organism, which makes completely resolving both spectra difficult. Table 3 displays the decay associated amplitude matrix calculated from the model in Fig. 6. PC645 is observed to transfer energy to PSII on a 100-ps timescale. Because PSI decays on a faster timescale (16 ps) than it becomes populated by PC645 (100 ps), a negative amplitude (population rise) is observed for PSI with a time constant of 16 ps and a positive amplitude (population decay) with a 100-ps time constant.

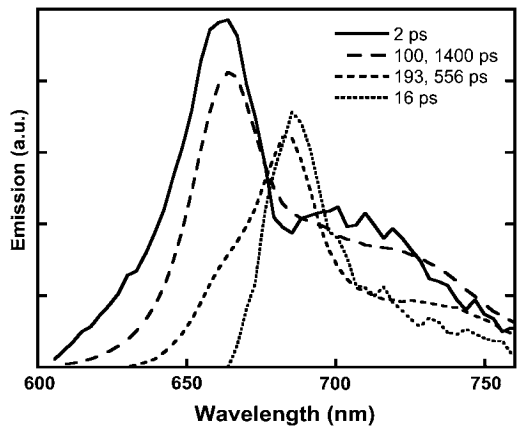

FIGURE 7 Species associated spectra of *Chroomonas* CCPM270 on 582 nm excitation according to the model in Fig. 6. The solid and long-dashed lines represent the emission of PC645 (662.5 and 664 nm), the short-dashed line is assigned to PSII (683.5 nm), and the dotted line is assigned to PSI (686.5 nm).

TABLE 3 Amplitude matrix for the different lifetimes associated with the target model of Fig. 6

	PC_1	PC_2	PC_3	$PSII_1$	$PSII_2$	PSI_1
τ (ps)	0.89 *hv**	–	–	0.066 *hv**	–	0.043 *hv**
2	0.89	−0.91	–	0.01	–	0.009
16	–	–	–	–	–	−0.041
100	–	0.91	−0.0051	−1.049	0.22	0.087
193	–	–	–	1.094	−0.55	–
556	–	–	–	–	0.33	–
1400	–	–	0.0051	–	–	–

Negative amplitude indicates a rise of excited state population and a positive amplitude a decay.
*Indicates the initial excitation ratio of the PC_1, PSI_1, and $PSII_1$ compartments.

The SAS estimated from the two intact algae experiments on 400 and 582 nm excitation were compared and showed nearly perfect overlap between the respective PC645 and PSII spectra (not shown) and their fluorescence lifetimes. In the 582 nm data analysis the PSI spectrum was, however, 2 nm blue-shifted with respect to that determined from the 400 nm data, which is due to the lack of resolution in the 582 nm experiment as mentioned before. The spectral lineshapes of PSI and PSII are also in close agreement with their respective SAS obtained from similar measurements on *Rhodomonas* CS24 algae (18).

Representative kinetic traces of the raw data and the fits are shown in Fig. 8. Data were obtained at three timebases of 200, 500, and 2000 ps, which have different instrument response functions of 5, 8, and 25 ps full width at half-maximum. respectively. When comparing the kinetic traces on 400 nm excitation (Fig. 8 *a*) with 582 nm excitation (Fig. 8 *b*), some differences that are reflected in the target analysis models can be seen. At 632 nm emission, the fast 2 ps energy transfer within PC645 can be seen in (Fig. 8 *b*) due to the large fraction of PC645 being directly excited by the laser pulses. At 632 nm emission, the traces in (Fig. 8 *a*) are noisy due to the relatively low PC645 excitation ratio at 400 nm compared to the photosystems. At 684 nm, fast trapping of excitations on PSI (40 ps) is observed in the 400 nm data (Fig. 8 *a*), though in the 582 nm data (Fig. 8 *b*) this decay is compensated by a slow rise by energy transfer from PC645, resulting in a plateau-shaped timetrace for the first 50 ps.

It is noted that the energy transfer rates from PC645 to the Chls of the respective photosystems I and II are 4.4 and 5.2 ns^{-1} (Table 1), which are of the same order as the estimated values of 4.2 and 3.5 ns^{-1} in *Rhodomonas* CS24 (18). In the latter experiment, measurements of time-resolved anisotropy facilitated the determination of energy transfer from PE545 to the photosystems in the membranes at faster rates up to 8.4 ns^{-1} as well. The kinetic information that can be extracted from the data using target analysis is limited. Because it became necessary to put spectral restrictions to resolve the PSI kinetics in the 582 nm data, it became impossible to determine more than a single energy transfer timescale for

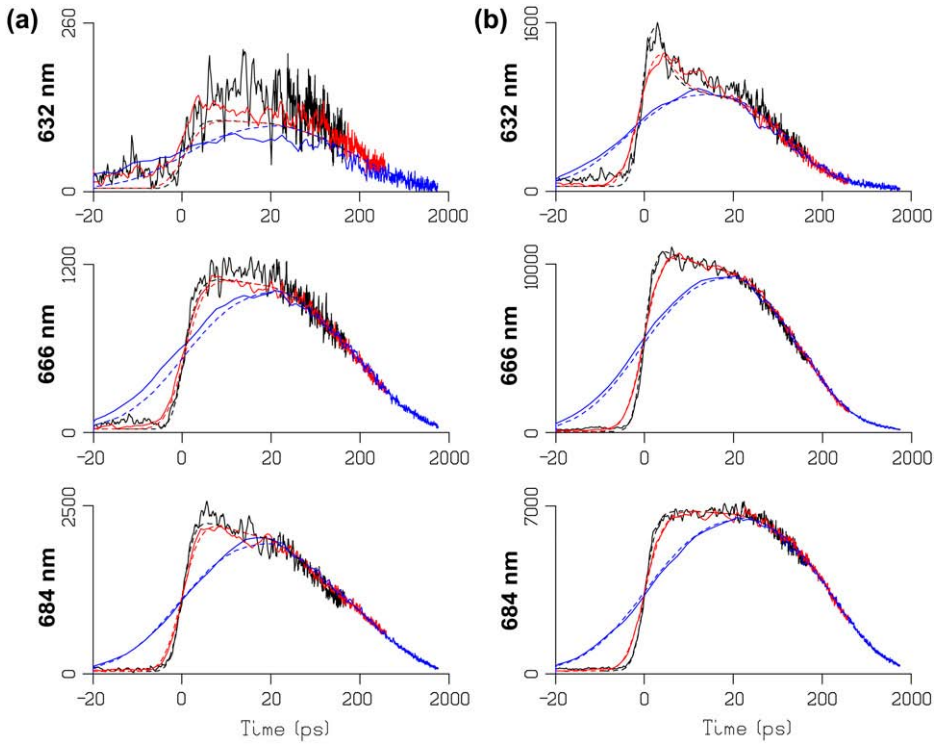

FIGURE 8 Selection of fluorescence decay time-traces and their fits of *Chroomonas* CCPM270 intact algae on 400 nm (*a*) and 582 nm (*b*) excitation according to the models displayed in Figs. 4 and 6. The solid lines represent the raw data, respectively measured at the timescales of 200 ps (*black*), 500 ps (*red*), and 2000 ps (*blue*); the dotted lines represent the fits. The time axis is linear for −20–20 ps relative to the instrument response functions maximum and logarithmic thereafter.

the excitations from PC645 to the Chls in the membrane. However, from the global analysis of the 582 nm data it was observed that PC645 to Chl *a* energy transfer also occurs at a timescale of 45 ps (Fig. 3 *c*). Thus, the fast energy transfer phases observed for *Rhodomonas* CS24 (18) will also be present in the data of *Chroomonas* CCMP270 in this study, but could not be resolved without anisotropic data.

PC645 has a high spectral overlap with Chl *a*, whereas PE545 shows good spectral overlap with both Chl *a* and *c2* (30). Consequently, comparison of their respective (Förster) energy transfer rates to the Chls in the membranes will be dependent largely on their respective distances to these Chls. The observed similar timescales of energy transfer from two spectrally different phycobiliproteins to the Chls of the photosystems suggests a similar membrane organization in both types of alga, which was suggested to show high similarity with plants and have the phycobiliproteins tightly packed in the lumen, around the periphery of the photosystems (18). Energy transfer then occurs from any of the peripheral bilin chromophores within PC645 to the Chls in the membrane. The 100 ps energy transfer time constant is then representative of a distribution of energy transfer timescales from PC645 to the photosystem Chls (35).

The energy distribution from phycobiliproteins to PSI and PSII is found to be rather similar for *Chroomonas* CCMP270 (~45:55) and *Rhodomonas* CS24 (54:46). The difference might be explained by different ratios of PSI and PSII present in the alga, which can also be caused by different growth conditions or to the binding of extra Chl *a*/*c2* antenna to PSII, which facilitates an increased rate of energy transfer, with respect to *Rhodomonas* CS24. Binding of extra antenna to PSII would also explain the observed blue-shift of the Chl emission maximum in *Chroomonas* CCMP270 (683 nm, Fig. 2) with respect to *Rhodomonas* CS24 (686 nm) (18).

CONCLUSIONS

On the basis of the global analysis of isolated PC645 excited at 582 nm, in combination with a target analysis of the algae excited both at 400 and 582 nm, it has been possible to develop a model of energy distribution on PC645 excitation in intact *Chroomonas* CCPM270 cells. Excitation energy from PC645 is transferred with high efficiency to PSI and PSII on a ~100-ps timescale, and respective ratio of ~45:55. The trap times of PSI (~30 ps) and PSII (200, ~500 ps) correspond to those obtained from experiments on isolated photosystems (44–51). The results illustrate the >99% efficiency of energy transfer from PC645 to the Chls in *Chroomonas* CCMP270, which is even better than the ~98% energy transfer efficiency estimated for PE545 in *Rhodomonas* CS24 (18).

ACKNOWLEDGMENTS

The research of VU-Biophysics was supported by The Netherlands Organization of Scientific Research via the foundation of Earth and Life Sciences and by the European Union (grant MRTN-CT-2003-505069, Intro2). C.D.W.W. was supported by The Netherlands Foundation for

Fundamental Research on Matter. A.B.D. was supported by the Intro2 network. P.M.G.C. and K.E.W. acknowledge grants from the Australian Research Council and the University of New South Wales.

REFERENCES

1. Bergmann, T. I. 2004. The physiological ecology and natural distribution patterns of cryptomonas algae in coastal aquatic ecosystems. PhD thesis. Rutgers, The State University of New Jersey, New Brunswick.
2. Macpherson, A. N., and R. G. Hiller. 2003. Algae with chlorophyll c. *In* Light-Harvesting Antennas in Photosynthesis. B. R. Green and W. W. Parson, editors. Kluwer Academic Publishers, Dordrecht, The Netherlands. 323–352.
3. Spear-Bernstein, L., and K. R. Miller. 1989. Unique location of the phycobiliprotein light-harvesting pigment in the cryptophyceae. *J. Phycol.* 25:412–419.
4. MacColl, R., and D. Guard-Friar. 1987. Phycobiliproteins. CRC Press, Boca Raton, FL.
5. Snyder, U. K., and J. Biggins. 1987. Excitation energy redistribution in the cryptomonad alga *Chryptomonas ovata*. *Biochim. Biophys. Acta.* 892:48–55.
6. Spear-Bernstein, L., and K. R. Miller. 1985. Are the photosynthetic membranes of cryptophyte algae inside out? *Protoplasma.* 129:1–9.
7. Kirk, J. 1994. Light and Photosynthesis in Aquatic Ecosystems. Cambridge University Press, Cambridge, UK.
8. Bruce, D., J. Biggins, T. Steiner, and M. Thewalt. 1986. Excitation energy transfer in the cryptophytes. Fluorescence excitation spectra and picosecond time-resolved emission spectra of intact algae at 77 K. *Photochem. Photobiol.* 44:519–525.
9. Lichtlé, C., H. Jupin, and J. Duval. 1980. Energy transfers from Photosystem II to Photosystem I in *Cryptomonas rufescens* (Cryptophyceae). *Biochim. Biophys. Acta.* 591:104–112.
10. Sidler, W. A. 1994. Phycobilisome and phycobiliprotein structures. *In* The Molecular Biology of Cyanobacteria. Advances in Photosynthesis, Vol. 1. D. A. Bryant, editor. Kluwer Academic Publishers, Dordrecht, The Netherlands. 139–216.
11. Mimuro, M., N. Tamai, A. Murakami, M. Watanabe, M. Erata, M. M. Watanabe, M. Tokutomi, and I. Yamazaki. 1998. Multiple pathways of excitation energy flow in the photosynthetic pigment system of a cryptophyte, *Cryptomonas* sp. (CR-1). *Phycol. Res.* 46:155–164.
12. Melis, A. 1989. Spectroscopic methods in photosynthesis—photosystem stoichiometry and chlorophyll antenna size. *Philos. Trans. R. Soc. Lond. B Biol. Sci.* 323:397–409.
13. Gantt, E. 1981. Phycobilisomes. *Ann. Rev. Plant Physiol. Plant Mol. Biol.* 32:327–347.
14. Lichtlé, C., J. C. Duval, and Y. Lemoine. 1987. Comparative biochemical functional and ultrastructural studies of photosytem particles from a cryptophycea: C*ryptomonas rufescens*; isolation of an active phycoerythrin particle. *Biochim. Biophys. Acta.* 894:76–90.
15. Haxo, F., and D. Fork. 1959. Photosynthetically active accessory pigments of cryptomonads. *Nature.* 184:1051–1052.
16. MacColl, R., L. E. Eisele, M. Dhar, J.-P. Ecuyer, S. Hopkins, J. Marrone, R. Barnard, H. Malak, and A. J. Lewitus. 1999. Bilin organization on cryptomonad biliproteins. *Biochemistry.* 28:4097–4105.
17. Wedemayer, G. J., D. E. Wemmer, and A. Glazer. 1991. Phycobilins of cryptophycean algae: structures of novel bilins with acryloyl substituents from phycoerythrin 566. *J. Biol. Chem.* 266:4731–4741.
18. Van der Weij-De Wit, C. D., A. B. Doust, I. H. M. Van Stokkum, J. P. Dekker, K. E. Wilk, P. M. G. Curmi, G. D. Scholes, and R. Van Grondelle. 2006. How energy funnels from the phycoerythrin antenna complex to photosystem I and photosystem II in cryptophyte *Rhodomonas* CS24 cells. *J. Phys. Chem. B.* 110:25066–25073.
19. Sidler, W., H. Nutt, B. Kumf, G. Frank, F. Suter, A. Brenzel, W. Wehrmeyer, and H. Zuber. 1990. The complete amino-acid sequence and the phylogenetic origin of phycocyanin-645 from the cryptophytan alga *Chroomonas* sp. *Biol. Chem. Hoppe Seyler.* 371:537–547.
20. Sidler, W., B. Kumpf, F. Suter, W. Morisset, W. Wehrmeyer, and H. Zuber. 1985. Structural studies on cryptomonad biliprotein subunits. Two different alpha-subunits in *Chroomonas* phycocyanin-645 and *Cryptomonas* phycoerythrin-545. *Biol. Chem. Hoppe Seyler.* 366:233–244.
21. Doust, A. B., K. E. Wilk, P. M. G. Curmi, and G. D. Scholes. 2006. The photophysics of cryptophyte light-harvesting. *J. Photochem. Photobiol. Chem.* 184:1–17.
22. Wedemayer, G. J., D. G. Kidd, D. E. Wemmer, and A. N. Glazer. 1992. Phycobilins of cryptophycean algae—occurrence of dihydrobiliverdin and mesobiliverdin in cryptomonad biliproteins. *J. Biol. Chem.* 267:7315–7331.
23. Mirkovic, T., A. B. Doust, J. Kim, K. E. Wilk, C. Curutchet, B. Mennucci, R. Cammi, P. M. G. Curmi, and G. D. Scholes. 2007. Ultrafast light harvesting dynamics in the cryptophyte phycocyanin 645. *Photochem. Photobiol. Sci.* 6:964–975.
24. Doust, A. B., I. H. M. Van Stokkum, D. S. Larsen, K. E. Wilk, P. M. G. Curmi, R. Van Grondelle, and G. D. Scholes. 2005. Mediation of ultrafast light-harvesting by a central dimer in phycoerythrin 545 studied by transient absorption and global analysis. *J. Phys. Chem. B.* 109:14219–14226.
25. Hiller, R. G., C. D. Scaramuzzi, and J. Breton. 1992. The organisation of photosynthetic pigments in a cryptophyte alga: a linear dichroism study. *Biochim. Biophys. Acta.* 1102:360–364.
26. Toole, C. M., and F. C. T. Allnutt. 2003. Red, cryptomonad and glaucocystophyte algal phycobiliproteins. *In* Photosynthesis in Algae. A. W. D. Larkum, S. E. Douglas, and J. A. Raven, editors. Kluwer Academic Publishers, Dordrecht, The Netherlands. 305–334.
27. Dekker, J. P., and E. J. Boekema. 2005. Supramolecular organization of thylakoid membrane proteins in green plants. *Biochim. Biophys. Acta.* 1706:12–39.
28. Lichtlé, C., J. C. Duval, N. Hauswirth, and A. Spilara. 1986. Freeze-fracture study of thylakoid organization of *Cryptomonas-rufescens* (cryptophyceae) according to illumination conditions. *Photobiochem. Photobiophys.* 11:159–171.
29. Hiller, R. G., and C. D. Martin. 1987. Multiple forms of a type I phycoerythrin from a *Chroomonas* sp. (Cryptophyceae) varying in subunit composition. *Biochim. Biophys. Acta.* 923:98–102.
30. MacColl, R., and D. S. Berns. 1978. Energy transfer studies on cryptomonad biliproteins. *Photochem. Photobiol.* 27:343–349.
31. Guillard, R. L., and J. H. Ryther. 1962. Studies of marine planktonic diatoms. I. *Cyclotella nana* and *Detonula confervacea*. *Can. J. Microbiol.* 8:229–239.
32. Gervais, F. 1997. Light-dependent growth, dark survival, and glucose uptake by cryptophytes isolated from a freshwater chemocline. *J. Phycol.* 33:18–25.
33. Scopes, R. K. 1987. Protein Purification, Principles and Practice, 2nd edition. Spring-Verlag, New York.
34. Gobets, B., I. H. M. Van Stokkum, M. Rögner, J. Kruip, E. Schlodder, N. V. Karapetyan, J. P. Dekker, and R. Van Grondelle. 2001. Time-resolved fluorescence emission measurements of photosystem I particles of various cyanobacteria: a unified compartment model. *Biophys. J.* 81:407–424.
35. Van Stokkum, I. H. M., D. S. Larsen, and R. Van Grondelle. 2004. Global and target analysis of time-resolved spectra. *Biochim Biophys Acta.* 1657:82–104. (Erratum in *Biochim Biophys Acta.* 2004. 1658:262).
36. Van Stokkum, I. H. M., B. van Oort, F. van Mourik, B. Gobets, and H. van Amerongen. 2008. Biophysical techniques in photosynthesis, Vol. 2. T. J. Aartsma and J. Matysik, editors. *In* Series Advances in Photosynthesis and Respiration, Vol. 26. Springer, Dordrecht, The Netherlands. 223–240.
37. Ingram, K., and R. G. Hiller. 1983. Isolation and characterization of a major chlorophyll a/c2 light-harvesting protein from a *Chroomonas* species (cryptophyceae). *Biochim. Biophys. Acta.* 722:310–319.
38. Harnischfeger, G., and B. Herold. 1981. Aspects of energy-transfer between phycobilins and chlorophyll in *Chroomonas* spec (cryptophyceae). *Ber. Dtsch. Bot. Ges.* 94:65–73.

39. Stón, J., and A. Kosakowska. 2002. Phytoplankton pigments designation—an application of RP-HPLC in qualitative and quantitative analysis. *J. Appl. Phycol.* 14:205–210.

40. Van der Weij-de Wit, C. D., J. A. Ihalainen, R. Van Grondelle, and J. P. Dekker. 2007. Excitation energy transfer in native and unstacked thylakoid membranes studied by low temperature and ultrafast fluorescence spectroscopy. *Photosynth. Res.* In press.

41. Andrizhiyevskaya, E. G., A. Chojnicka, J. A. Bautista, B. A. Diner, R. Van Grondelle, and J. P. Dekker. 2005. Origin of the F685 and F695 fluorescence in photosystem II. *Photosynth. Res.* 84:173–180.

42. Malak, H., and R. MacColl. 1991. A picosecond time-resolved fluorescence study on the biliprotein, phycocyanin 645. *Biochim. Biophys. Acta.* 1059:165–170.

43. Holzwarth, A. R., J. Wendler, and W. Wehrmeyer. 1983. Studies on chromophore coupling in isolated phycobiliproteins. I. Picosecond fluorescence kinetics of energy transfer in phycocyanin 645 from *Chroomonas* sp. *Biochim. Biophys. Acta.* 724:388–395.

44. Andrizhiyevskaya, E. G., D. Frolov, R. Van Grondelle, and J. P. Dekker. 2004. On the role of the CP47 core antenna in the energy transfer and trapping dynamics of photosystem II. *Phys. Chem. Chem. Phys.* 6:4810–4819.

45. Van Amerongen, H., and J. P. Dekker. 2003. Light-harvesting antennas in photosynthesis. *In* Advances in Photosynthesis and Respiration. B. R. Green and W. W. Parson, editors. Kluwer Academic Publishers, Dordrecht, The Netherlands. 219–251.

46. Van Mieghem, F. J. E., G. F. W. Searle, A. W. Rutherford, and T. J. Schaafsma. 1992. The influence of the double reduction of Q_A on the fluorescence decay kinetics of photosystem II. *Biochim. Biophys. Acta.* 1100:198–206.

47. Broess, K., G. Trinkunas, C. D. Van der Weij-de Wit, J. P. Dekker, A. Van Hoek, and H. Van Amerongen. 2006. Excitation energy transfer and charge separation in photosystem II membranes revisited. *Biophys. J.* 91:3776–3786.

48. Ihalainen, J. A., P. E. Jensen, A. Haldrup, I. H. M. Van Stokkum, R. Van Grondelle, H. V. Scheller, and J. P. Dekker. 2002. Pigment organization and energy transfer dynamics in isolated photosystem I (PSI) complexes from *Arabidopsis thaliana* depleted of the PSI-G, PSI-K, PSI-L, or PSI-N subunit. *Biophys. J.* 83:2190–2201.

49. Gobets, B., and R. Van Grondelle. 2001. Energy transfer and trapping in photosystem I. *Biochim. Biophys. Acta.* 1507:80–99.

50. Croce, R., D. Dorra, A. R. Holzwarth, and R. C. Jennings. 2000. Fluorescence decay and spectral evolution in intact photosystem I of higher plants. *Biochemistry.* 39:6341–6348.

51. Ihalainen, J. A., I. H. M. Van Stokkum, K. Gibasiewicz, M. Germano, R. Van Grondelle, and J. P. Dekker. 2005. Kinetics of excitation trapping in intact photosystem I of *Chlamydomonas reinhardtii* and *Arabidopsis thaliana*. *Biochim. Biophys. Acta.* 1706:267–275.